5464–5471 *Nucleic Acids Research, 1998, Vol. 26, No. 23*

A novel end-to-end binding of two netropsins to the DNA decamers d(CCCCCIIIII)$_2$, d(CCCBr^{5}CCIIIII)$_2$ and d(CBr^{5}CCCCIIIII)$_2$

X. Chen, S. N. Mitra, S. T. Rao, K. Sekar and M. Sundaralingam*

The Ohio State University, Biological Macromolecular Structure Center, Departments of Chemistry and Biochemistry, 012 Rightmire Hall, 1060 Carmack Road, Columbus, OH 43210, USA

Received July 15, 1998; Revised and Accepted October 9, 1998

NDB accession nos+

ABSTRACT

Netropsin is bound to the DNA decamer d(CCCCCIIIII)$_2$, the C-4 bromo derivative d(CCCBr^{5}CCIIIII)$_2$ and the C-2 bromo derivative d(CBr^{5}CCCCIIIII)$_2$ in a novel 2:1 mode. Complexes of the native decamer and the C-4 bromo derivative are isomorphous, space group P1, unit cell dimensions *a* = 32.56 Å (32.66), *b* = 32.59 Å (32.77), *c* = 37.64 Å (37.71), α = 86.30° (86.01°), β = 84.50° (84.37°), γ = 68.58° (68.90°) with two independent molecules (A and B) in the asymmetric unit (values in parentheses are for the derivative). The C-2 bromo derivative is hexagonal P6$_1$, unit cell dimensions *a* = *b* = 32.13 Å, *c* = 143.92, γ = 120° with one molecule in the asymmetric unit. The structures were solved by the molecular replacement method. The novelty of the structures is that there are two netropsins bound end-to-end in the minor groove of each B-DNA decamer which has nearly a complete turn. The netropsins are held by hydrogen bonding interactions to the base atoms and by sandwiching van der Waal's interactions from the sugar–phosphate backbones of the double helix similar to every other drug·DNA complex. Each netropsin molecule spans ~5 bp. The netropsins refined with their guanidinium heads facing each other at the center, although an orientational disorder for the netropsins cannot be excluded. The amidinium ends stretch out toward the junctions and bind to the adjacent duplexes in the columns of stacked symmetry-related complexes. Both cationic ends of netropsin are bridged by water molecules in one of the independent molecules (molecule A) of the triclinic structures and also the hexagonal structure to form pseudo-continuous drug·decamer helices.

INTRODUCTION

The antiviral antitumor antibiotics netropsin (Fig. 1) and distamycin are amongst the minor groove binding drugs which form complexes with A·T/I·C specific sequences of DNA (1–6). The first crystal structure of a drug–DNA complex was that of a 1:1 complex of the dodecamer (CGCGAATTBr^{5}CGCG) with netropsin (7). This was followed by several crystal structures of the isomorphous 1:1 complexes, namely distamycin (8), Hoechst 33258 (9,10), berenil (11), 4′-6-diamidine-2-phenylindole (DAPI) (12–14), pentamidine (15) and propamidine (16). Later, the crystal structure of a new side-by-side 2:1 binding of distamycin to an alternating octamer DNA d(ICICICIC) was reported (17). The same 2:1 binding mode had been observed in solution for an undecamer by NMR a few years earlier (18). The side-by-side binding was retained when the I·C base pairs were progressively replaced by A·T base pairs (19) or when one or more of the cytidines were replaced by ribocytidines to give a DNA–RNA chimera (20). Synthetic analogs of distamycin are also known to form side-by-side complexes in solution (21,22) as well as in crystals (23,24).

Thus the natural drugs netropsin and distamycin exhibit a 1:1 binding to DNA while distamycin also exhibits a 2:1 side-by-side binding. We have continued the studies with a longer decamer sequence instead of the octamer d(ICICICIC)$_2$ with both netropsin and distamycin but neither gave crystals. Therefore, the homopyrimidine·homopurine decamer sequence d(CCCCCIIIII) was synthesized for complexation with netropsin and distamycin. Suitable crystals were obtained with netropsin but not with distamycin. It may be mentioned that all the 2:1 side-by-side complexes of distamycin are with alternating purine·pyrimidine octamers. Dicationic netropsin should be able to form 2:1 side-by-side complexes like monocationic distamycin, where the two netropsins can be staggered to avoid charge repulsion, but so far no such complex has been obtained. Five mono-bromocytosine derivatives (C1–C5) were synthesized but only the C-4 bromo derivative yielded isomorphous crystals. The C-2 bromo derivative (hexagonal, P6$_1$) also gave suitable diffracting crystals. Here we report the crystal structures of netropsin complexes of the decamers: the native and the C-4 bromo and the C-2 bromo analogs.

MATERIALS AND METHODS

Synthesis, crystallization and data collection

All three DNA sequences were synthesized by the solid phase phosphoramidite method on an Applied Biosystems 381 DNA

*To whom correspondence should be addressed. Tel: +1 614 292 2925; Fax: +1 614 292 2524; Email: sundaral@chemistry.ohio-state.edu

+GDJ059, GDJB58 and GDJB55

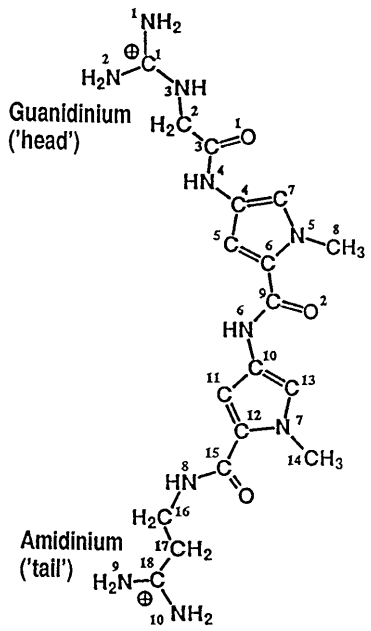

Figure 1. Chemical structure and atom numbering of netropsin. The guanidinium and amidinium groups at either end are positively charged and labeled as head and tail, respectively.

synthesizer. Crystallization experiments were done by the hanging drop vapor diffusion technique. The native compound was crystallized from a droplet containing 0.3 mM oligonucleotide (single strand concentration), 0.3 mM netropsin, 0.4 mM sodium cacodylate buffer (pH 6) and 0.06 mM cobaltic hexamine chloride equilibrated against 60% 2-methyl-2,4-pentanediol at room temperature (291 K). Light yellow crystals, up to 1.0 × 0.3 × 0.1 mm in size, appeared in a few weeks. The C-4 bromo and the C-2 bromo compounds were crystallized with slight variation in the crystallization conditions.

X-ray diffraction data were collected at room temperature using an R-AXIS IIc imaging plate system equipped with a Rigaku copper rotating anode and a graphite monochromator (CuK_α, λ = 1.5418 Å). The frames were processed using the software from Molecular Structure Corporation. The crystallographic data are summarized in Table 1. Meridional reflections of 3.4 Å were observed along the *a* and *b* axes for the native as well as the bromo analogs indicating that they were in the B-DNA conformation.

Structural solution

The four independent bromine atoms corresponding to two independent duplexes were readily located in the difference Patterson map between the native and the C-4 bromo complexes. Attempts to solve the structure of the native complex using the iterative single isomorphous replacement method (25) failed, probably due to the low triclinic crystal symmetry. Hence the native structure was solved by the molecular replacement method using the program X-PLOR 3.1 (26) and fiber B-DNA as the search model (27). The C-4 bromo complex had the same structure as the native. The correctness of the structure was confirmed by the four bromine atoms. The structure of the C-2 bromo complex was also solved by the molecular replacement method but using the program AMoRe (28) and the coordinates of the native decamer as the search model. The correctness of the structure was again confirmed by the two bromine positions.

Table 1. Crystallographic data and refinement statistics for the native and the C-4 and C-2 bromo derivatives

	d(CCCCCIIIII)$_2$		d(CCCBr^{5}CCIIIII)$_2$		d(CBr^{5}CCCCIIIII)$_2$	
Crystallographic data						
Space group	P1		P1		P6$_1$	
Cell dimensions						
a (Å) α (°)	32.56	86.30	32.66	86.01	32.13	90.0
b β	32.59	84.50	32.77	84.37	32.13	90.0
c γ	37.64	68.58	37.71	68.90	143.92	120.0
Data resolution (Å)	2.4		2.4		2.5	
No. of unique reflections	4316 [2.8σ(F)]		4284 [2.8σ(F)]		1746 [2.0σ(F)]	
R_{sym}	0.045		0.061		0.059	
Refinement results						
No. of reflections used	3714 (F ≥ 4σ)		3883 (F ≥ 4σ)		1667 [F ≥ 2σ(F)]	
No. of water molecules	49		38		38	
Final R factor (R_{free})	0.190 (0.273)		0.199 (0.292)		0.211 (0.298)	
r.m.s. deviations from ideal geometry (parameter file: param_nd.dna)						
Bond length (Å)	0.014		0.015		0.008	
Bond angle (°)	2.6		2.7		1.7	
Dihedral angle (°)	18.7		18.8		21.2	
Improper angle (°)	1.7		1.81		1.4	

Refinement

Native triclinic complex. The refinement of the native triclinic complex was carried out using X-PLOR 3.1 (26). Five percent of the reflections were set aside for R_{free} calculation (29). The model building was done using the program CHAIN (30). The model was refined by several cycles of rigid body refinement, treating the two independent duplexes as separate rigid units, to an R_{work}/R_{free} of 0.42/0.49. The R_{work}/R_{free} dropped to 0.286/0.378 after Powell conjugate gradient energy minimization, followed by simulated annealing and individual B factor refinement to 0.286/0.378. The $|F_0| - |F_c|$ difference electron density maps (not shown) showed strong elongated crescent-shaped densities one behind the other (at the 2σ level) at two positions in the minor grooves of the independent duplexes. We placed a string of 12 water molecules at these difference densities for refinement. However, the R_{work}/R_{free} dropped marginally to 0.281/0.376 and also residual electron densities appeared at and near the sites of the string of water molecules. We therefore concluded that the difference densities were for two netropsin molecules. At each site two orientations were possible for the netropsins giving 16 possible combinations in the two duplexes. The netropsins could be fitted into the residual electron density in the minor groove of the two decamer duplexes in both orientations due to the quasi two-fold symmetry of the netropsin molecule. In one of the two orientations the netropsin methylpyrrole rings appeared to fit better; however, an orientational disorder could not be ruled out. We refined three models independently with identical parameters, one in which the netropsin head groups faced each other at the center of the duplexes, the other in which the tails faced each other and the third involving disordered netropsins in both orientations with 50% occupancies. R_{work}/R_{free} values were 0.232/0.309, 0.236/0.312 and 0.235/0.312, respectively, for the three models and netropsin orientations could not be distinguished. Refinement with all other possible orientational combinations gave similar R_{work}/R_{free}. Due to the low ratio of reflections/parameters, the disordered model was not further refined. The head-to-head orientation was chosen for further refinement, though it might be mentioned that other orientations cannot be excluded at this resolution. The terminal charged ends of the drugs are not in contact; the only close approach is in molecule B, where the N9 and N10 atoms of the two amidinium groups are 2.93 Å apart (Table 2). After 59 water molecules from difference electron density maps were incorporated into the model in four steps, the R_{work}/R_{free} for all 3714 reflections was 0.190/0.273.

Triclinic C-4 bromo complex. The triclinic C-4 bromo complex was refined starting with the DNA atoms of the native. The initial R_{work}/R_{free} was 0.287/0.39 for 3883 reflections at 2.4 Å resolution. A difference electron density map gave four bromine atoms at heights ranging from 6 to 8σ. The structure, including the bromine atoms, was subjected to simulated annealing followed by positional and B factor refinement, resulting in an R_{work}/R_{free} of 0.266/0.378. The difference electron density map again showed crescent-shaped electron densities in the minor grooves of both the duplexes, confirming the binding of two netropsins. As in the isomorphous native structure, the netropsins were placed in the head-to-head orientation. The refinement dropped R_{work}/R_{free} to 0.216/0.324. A total of 38 solvent sites were located. The final R_{work}/R_{free} was 0.199/0.292. A summary of refinement results is given in Table 1.

Table 2. Distances between the two charged ends of the netropsin molecules[a]

Atoms		Native complex[b]		C-2 bromo complex
Netropsin 1	Netropsin 2	Molecule A Distance (Å)	Molecule B Distance (Å)	Distance (Å)
N1	N1	5.50	6.65	8.45
N1	N2	5.60	5.19	6.50
N2	N1	5.37	7.30	7.07
N2	N2	4.47	6.26	4.88
N9	N9	5.80	5.19	4.52
N9	N10	4.96	2.93	5.88
N10	N9	7.34	4.91	5.52
N10	N10	7.01	3.37	6.95

[a]The distances of the charged ends to the bridged water are given in Figure 3.
[b]The distances in the C-4 bromo complex are almost identical to the native complex.

Hexagonal C-2 bromo complex. The hexagonal C-2 bromo complex was refined by the rigid body protocol of X-PLOR 3.1 (26) using all 1667 reflections between 8 and 2.5 Å; 10% were set aside for R_{free} (29). The R_{work}/R_{free} was 0.46/0.53. The two bromine atoms were added from the difference density maps. Refinement by Powell conjugate gradient energy minimization, simulated annealing and individual B factors and addition of 28 water molecules away from the minor groove dropped the R_{work}/R_{free} to 0.26/0.34. A difference Fourier map at this stage showed quite clearly the electron densities for the two netropsin molecules. They could be fitted into the density in four relative orientations. The head-to-head orientation here gave a slightly better fit, particularly for one of the pyrrole methyl groups (Fig. 2), but still the possibility of disorder cannot be ruled out. In the head-to-head orientation the two drug molecules were refined with the decamer duplex and 38 solvent molecules dropping the R_{work}/R_{free} to 0.211/0.298. There are no short contacts between the charged ends of the drugs (Table 2).

Coordinate sets and structure factors for all the three structures have been deposited with the Nucleic Acid Database (31), accession nos GDJ059, GDJB58 and GDJB55, respectively.

RESULTS

Novel netropsin–DNA complex

The structure analysis in two different crystal forms revealed that the novel netropsin–DNA complex contains two independent molecules in the asymmetric unit for the native and the isomorphous C-4 bromo compound but only one molecule for the hexagonal C-2 bromo compound. The two isomorphous structures are similar and therefore the detailed discussion is based on the native and the hexagonal C-2 bromo compounds. In each of the duplexes two drugs are bound in an end-to-end fashion almost filling the entire minor groove of the decamer. The decamer duplexes with 10.0 bp/turn for molecule A and 10.1 bp/turn for molecule B of the native and 10.1 bp/turn for the C-2 bromo compound resemble the canonical B-DNA. The r.m.s. atomic deviation on superimposition for the two independent duplexes of the asymmetric unit is 0.46 Å, while it is 0.72 Å for duplex A of the native and C-2 bromo compound and 0.90 Å for duplex B and the C-2 bromo compound. The average twist and rise for duplex

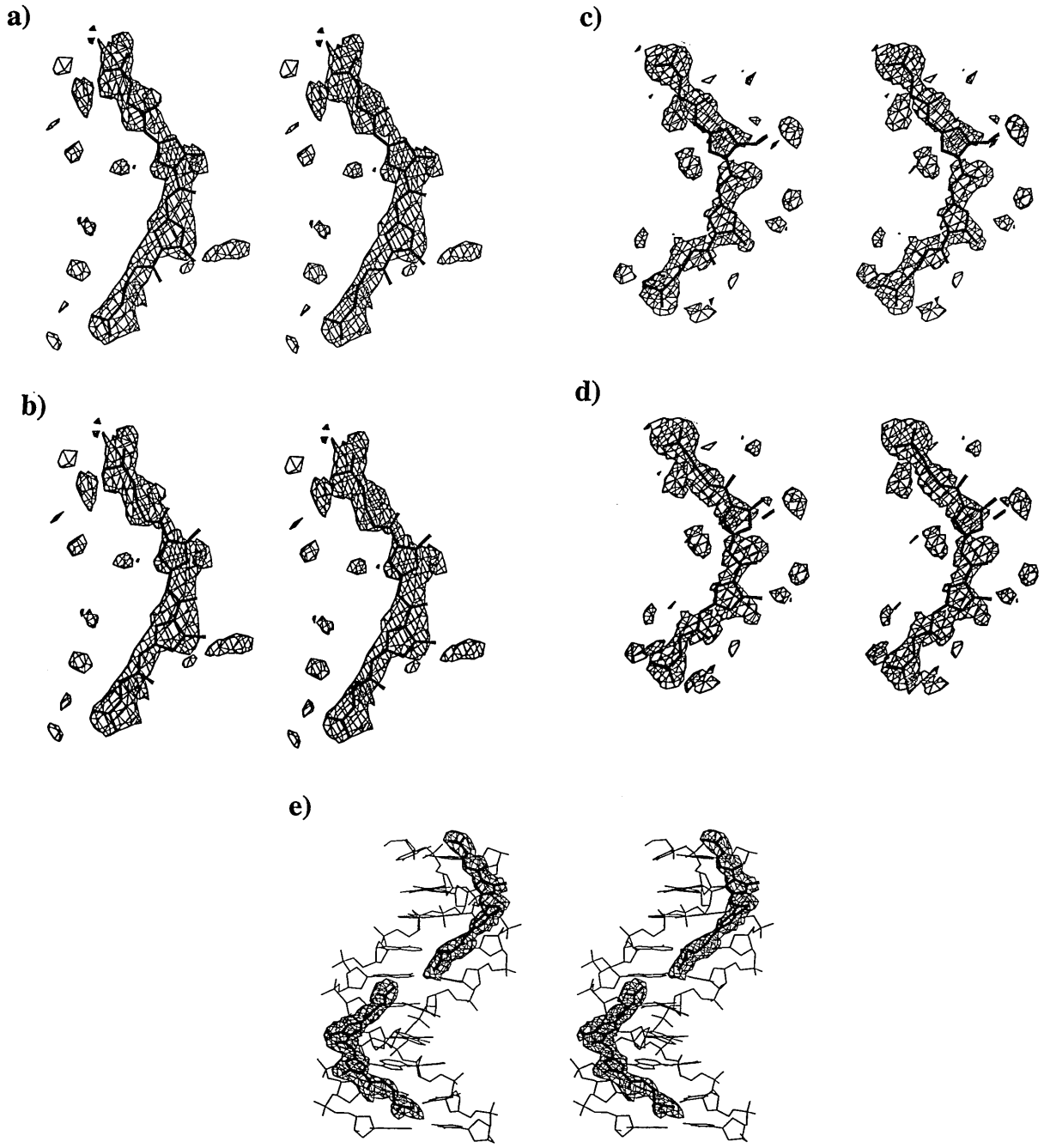

Figure 2. Stereoviews of the $|F_0| - |F_c|$ electron density maps contoured at 2.0σ in the C-2 bromo complex corresponding to the two netropsin molecules bound in the minor groove before they were included in the refinement. Netropsin A1 is shown in (**a**) and (**b**) in the two different orientations, while netropsin A2 is shown in (**c**) and (**d**) again in two orientations. As can be seen, the density maps cannot unambiguously distinguish the orientations of the netropsins and consequently disorder could not be ruled out. It may, however, be noted that a methyl group of netropsin seems to fit better in (a) and (c) corresponding to head-to-head binding of two drugs. (**e**) The final omit $2|F_0| - |F_c|$ electron density (at 1.0σ) for the netropsins.

A are 35.9°, 3.30 Å; for duplex B 35.7°, 3.26 Å and for the C-2 bromo compound 35.6°, 3.25 Å, respectively. The volumes per base pair are 1850 and 2150 $Å^3$ for the native and the C-2 bromo compounds, respectively, compared with 1100–1650 $Å^3$ in known oligonucleotide duplexes, and therefore the molecules are loosely packed in the crystals.

End-to-end binding

In each model duplex two netropsins are bound in the minor groove in single file with each drug spanning 5 bp. Assuming that the drugs are bound in the head-to-head orientation, the amidinium ends of the netropsins stretch slightly across the

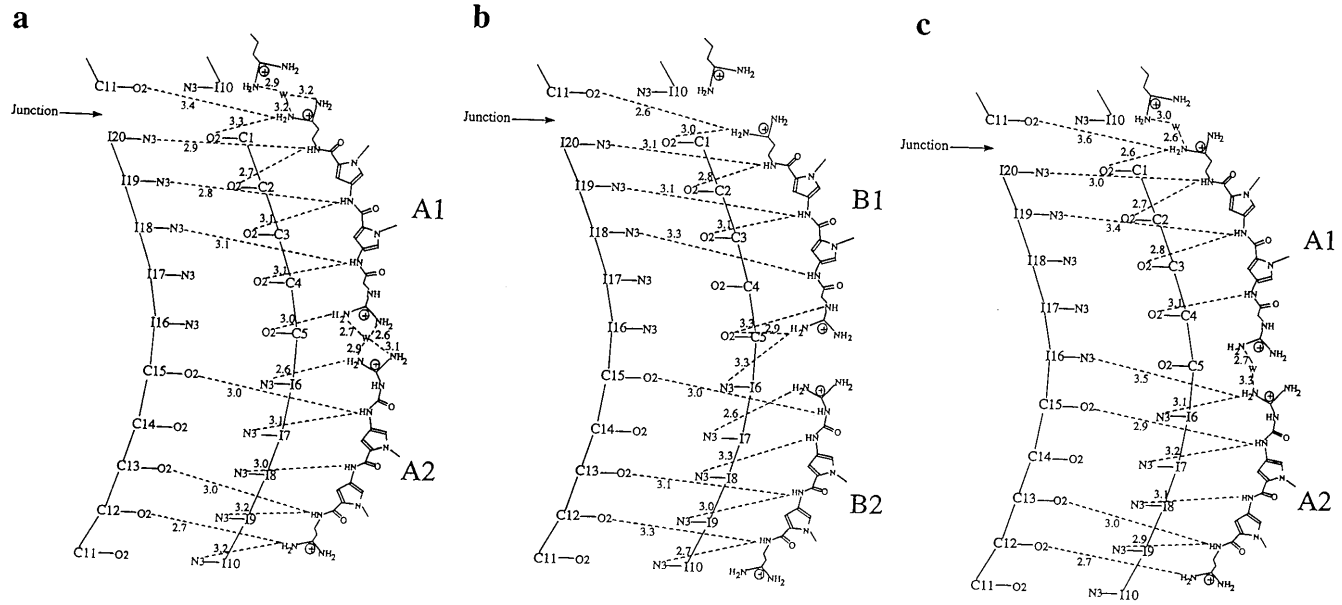

Figure 3. Hydrogen bonding interaction between the drugs and the DNA. (**a**) Molecule A of the native triclinic complex. (**b**) Molecule B of the native triclinic complex. (**c**) Hexagonal C-2 bromo complex.

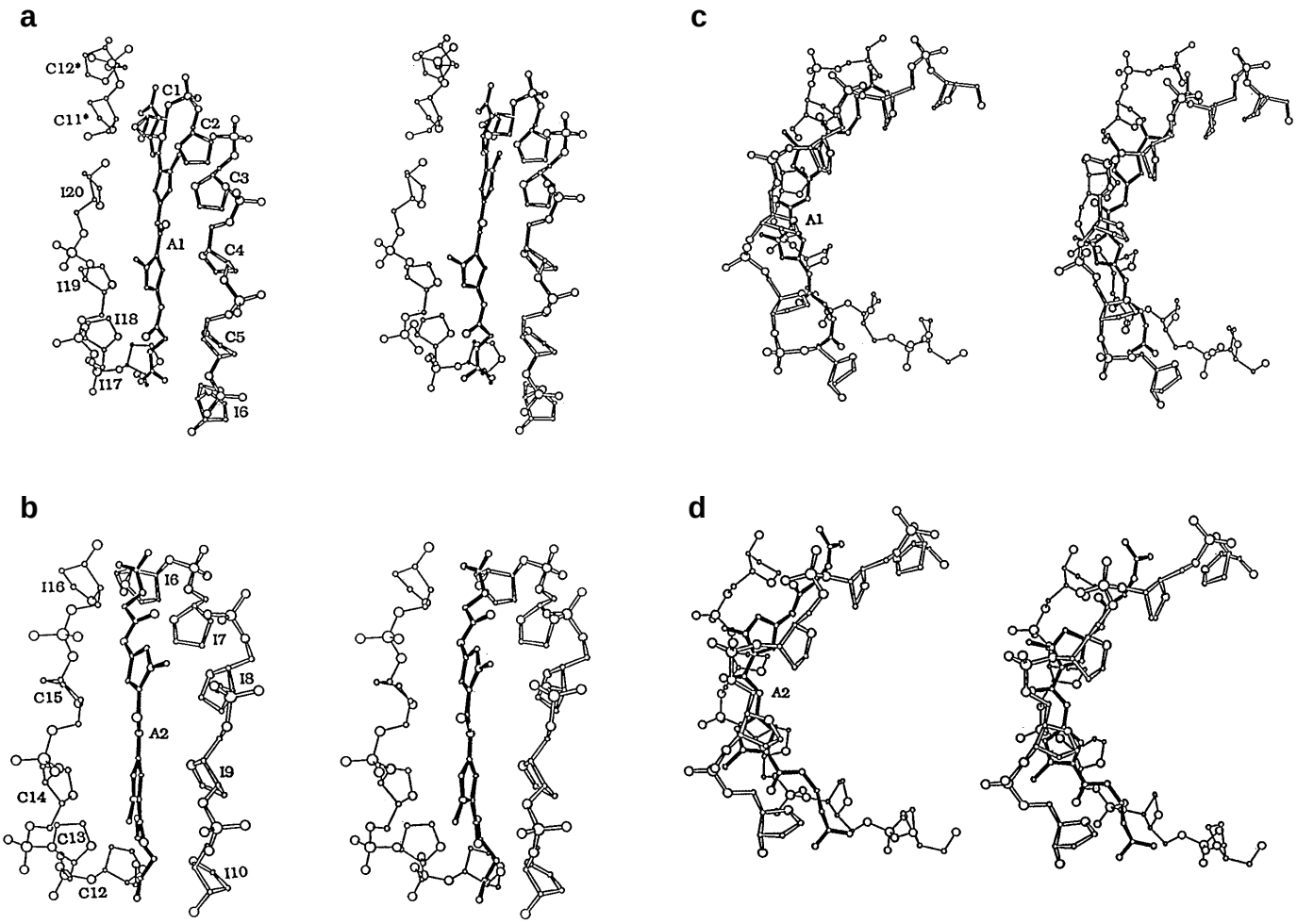

Figure 4. Representative diagrams showing the sandwiching van der Waals interactions between the drug and the DNA. Minor groove view of the C-2 bromo complex showing (**a**) netropsin A1 (asterisks indicate residues from translated molecule) and (**b**) netropsin A2. Same structure shown edge on for (**c**) netropsin A1 and (**d**) netropsin A2.

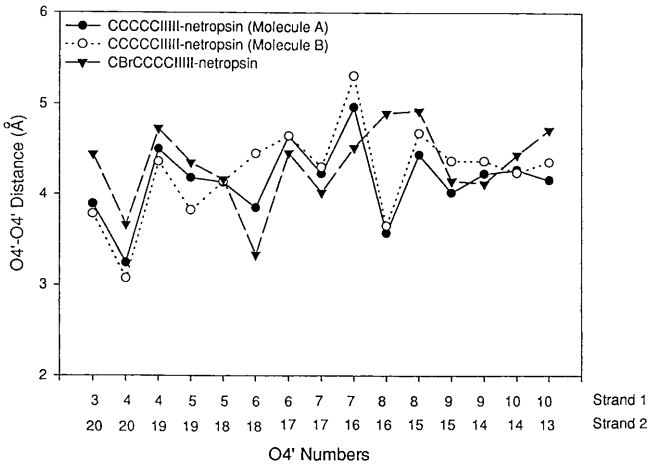

Figure 5. Minor groove widths measured by O4′–O4′ distances (less 2.8 Å for the two oxygen radii).

junctions and form hydrogen bonds to the terminal base pairs of neighboring duplexes (Fig. 3). The guanidinium groups are between cytosines 4 and 5 in duplex A of the triclinic structure. The same holds for the drug binding in the hexagonal structure with one molecule in the asymmetric unit. However, netropsin molecule B2 is slightly downshifted by ~1 bp compared with netropsin A2. The netropsin amide groups are located approximately midway between base pairs and engage in bifurcated hydrogen bonds to the O2 atoms of cytosine and N3 atoms of inosine. In this regard it is similar to the 1:1 complexes (13,14,32). The terminal amidinium groups of netropsins A1 and B1 in the triclinic and A1 in the hexagonal complexes are involved in bifurcated hydrogen bonds to two cytosine O2 atoms at the junction.

In the drug–minor groove complexes, van der Waals interactions between the sandwiching sugar–phosphate backbone chains and the drug play a major role in the stability of the complexes. There are a large number of short van der Waals contacts between the sugar ring O4′ and the phosphate backbone atoms and the π electrons of the methylpyrrole rings (13). Similar contacts have been found previously between the sugar O4′ atom and the nucleic acid bases (33,34), as shown in Figure 4. Water molecules bridge the two netropsin drugs in molecule A (but not molecule B) of both the triclinic and hexagonal structures (Fig. 4).

Minor groove widths

The minor groove widths for the decamers measured by the O4′–O4′ separations (35) are quite narrow throughout (Fig. 5). The P–P separations in the triclinic complex are consistently higher (0.4–2.0 Å) than the O4′–O4′ separations. Figure 5 shows the plot of minor groove widths for molecules A and B of the triclinic complex and the C-2 bromo compound and varies between 3.9 and 4.6, 3.7 and 4.8 and 3.9 and 4.6 Å respectively. The effect of drug binding on the minor groove width could not be discerned since the decamer without netropsin could not be crystallized.

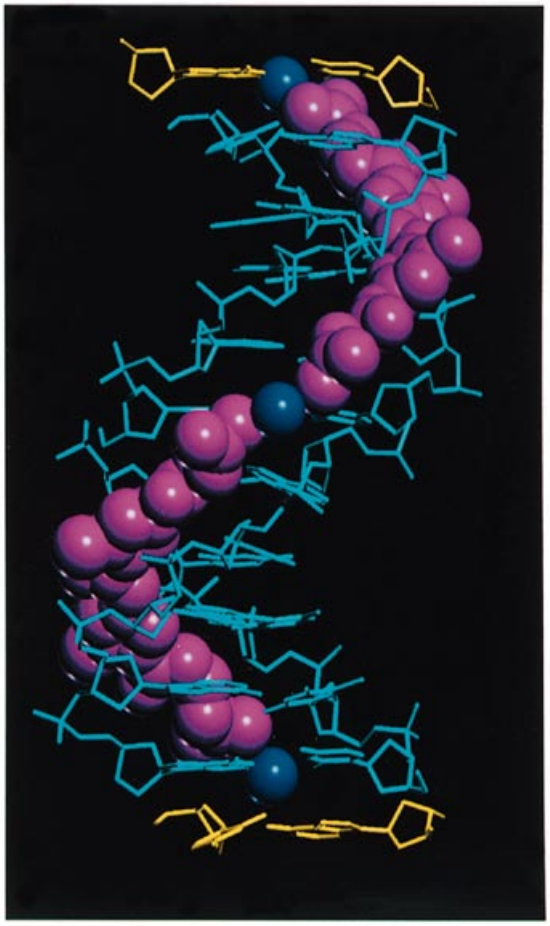

Figure 6. A representative color drawing for the complexes. Color coding: DNA, cyan; netropsins, purple; water molecules, blue. The bottom water molecule is related by translation to the upper water. In molecule B of the triclinic complex the water molecule at the middle of the drugs does not bridge the drugs.

DNA helical parameters

A representative color drawing of the crystal structures of the complexes is shown in Figure 6. The central CI steps have large helical twist angles, 39°, 38° and 42° for molecules A and B of the native structure and the hexagonal structure, respectively, while the flanking steps (C-C and I-I) have smaller values (average 31.3°). High twist angles (40.0°) are again found at the junction CI steps of the duplexes with a rise of 2.7 Å. All three sequences showed high propeller twists for the base pairs (average –14° and –15° for molecules A and B of the triclinic complexes and –16° for the hexagonal complex). The parameters were calculated by the NEWHEL92 program (36).

Hydration and crystal packing

The minor groove of the DNA is covered by the two netropsin drugs and is virtually dry to solvent molecules. Water molecules are found to bridge the drugs linking the guanidinium and the amidinium ends except in molecule B of the native complex. Most of the water molecules have direct contacts with the DNA; nearly half are hydrogen bonded to the major groove atoms and

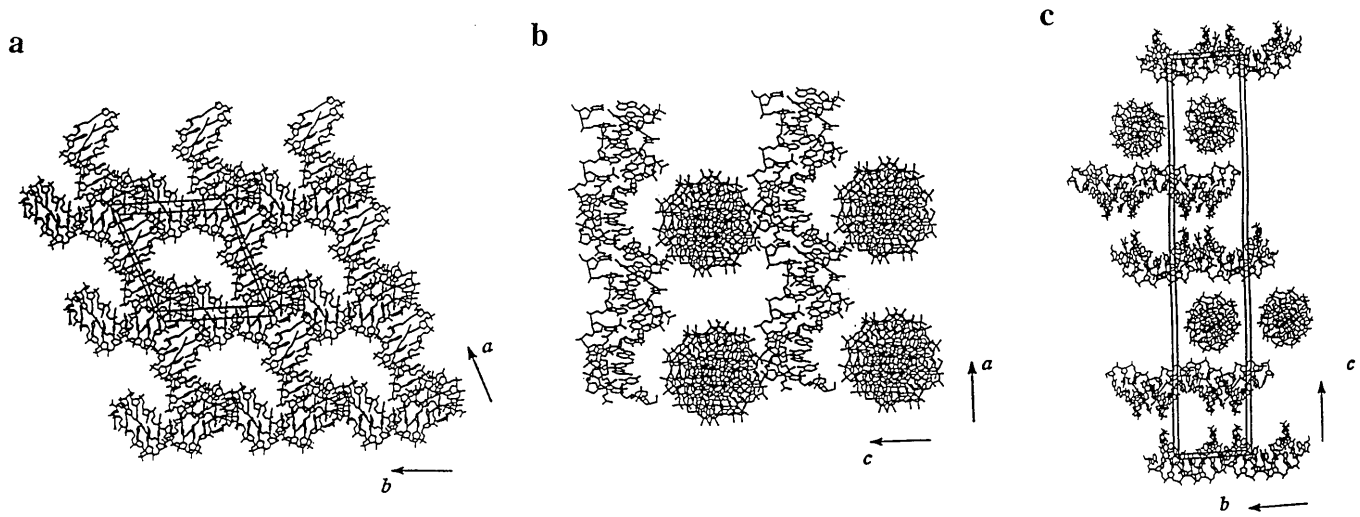

Figure 7. The crystal packing viewed down (**a**) the *c*-axis and (**b**) the *b*-axis for the triclinic complex and (**c**) for the C-2 bromo complex. Notice the pseudo-continuous columns of the decamers, running parallel to the *a* and *b* axes.

the other half to the phosphates. The drug–decamer complexes form pseudo-continuous helical columns with other molecules related by translation along the *a* and *b* axes (Fig. 7).

DISCUSSION

The aim of this study was to investigate whether netropsin can bind to a longer target sequence of DNA in the 2:1 side-by-side fashion. However, the present sequences displayed a 2:1 end-to-end binding for netropsin. The structural features of this mode of drug binding closely resemble the 1:1 drug–DNA complexes, e.g. bifurcated hydrogen bonding interactions between the amides of the drugs and the O2/N3 base atoms of the DNA, a significant narrowing of the minor groove and a run of high propeller twisted base pairs (similar to the A·T base pairs of 1:1 complexes). This is the first crystal structure of a homopyrimidine·homopurine sequence which shows two netropsins binding the whole length of the decamer sequence in a 2:1 ratio with one netropsin spanning 5 bp. While netropsin binding is in the end-to-end mode, distamycin binds in the side-by-side fashion. Studies on the side-by-side complexes of distamycin in this laboratory indicated that in this mode of binding the pyrrole carboxamide stacks of the two drugs contribute to the stability. Six pyrrole carboxamide stacks are possible for distamycin but only four for netropsin. Since netropsin has two positively charged end groups, a balance should be struck between stacking and charge repulsion to provide stability of the side-by-side complex. The fact that netropsins prefer to bind in an end-to-end fashion and not in the side-by-side fashion indicates that both stacking as well as the charges on the drugs are important in selecting the mode of binding. The importance of drug charges (monocationic or dicationic) in forming side-by-side complexes has been demonstrated in the lexitropsin–DNA complex (23). It appears that complexes with dicationic drugs (e.g. netropsin) form a single file as in the 2:1 end-to-end or 1:1 complexes while complexes with monocationic drugs (e.g. distamycin and lexitropsins) form side-by-side complexes. This hypothesis can be checked further by designing distamycin analogs as dications, either by changing the formyl amide group to a guanidinium or some other group. Such studies might throw more light on the influence of charge on drug–DNA complexes.

ACKNOWLEDGEMENTS

This work was supported by NIH grant GM-17378 and an Ohio Regents Eminent Scholar endowment. Partial financial support by the Hayes Investment Fund of the University for acquiring the R-axis IIc instrument is gratefully acknowledged. M.S. gratefully thanks the Ohio Board of Regents for an Eminent Scholar Chair.

REFERENCES

1 Reinert,K.E. and Thrum,H. (1970) *Stud. Biophys.*, **24/25**, 319–325.
2 Luck,G., Triebel,H., Waring,M. and Zimmer,Ch. (1974) *Nucleic Acids Res.*, **1**, 503–530.
3 Zasedatelev,A.S., Gursky,G.V., Zimmer,Ch. and Thrum,H. (1974) *Mol. Biol. Rep.*, **1**, 3337–3342.
4 Wartell,R., Larson,J.E. and Wells,R.D. (1974) *J. Biol. Chem.*, **249**, 6710–6731.
5 Van Dyke,M.W., Hertzberg,R.P. and Dervan,P.B. (1982) *Proc. Natl Acad. Sci. USA*, **79**, 5470–5474.
6 Zimmer,C. and Wahnert,U. (1986) *Prog. Biophys. Mol. Biol.*, **47**, 31–112.
7 Kopka,M.L., Yoon,C., Goodsell,D., Pjura,P. and Dickerson,R. (1985) *Proc. Natl Acad. Sci. USA*, **82**, 1376–1380.
8 Coll,M., Frederick,C.A., Wang,A.H.-J. and Rich,A. (1987) *Proc. Natl Acad. Sci. USA*, **84**, 8385–8389.
9 Pjura,P.E., Grzeskowiak,K. and Dickerson,R.E. (1987) *J. Biol. Chem.*, **197**, 257–271.
10 Teng,M.-K., Usman,N., Frederick,C.A. and Wang,A.H.-J. (1988) *Nucleic Acids Res.*, **16**, 2671–2690.
11 Brown,D.G., Sanderson,M.R., Skelly,J.V., Jenkins,T.C., Brown,T., Garman,E., Stuart,D.I. and Neidle,S. (1990) *EMBO J.*, **9**, 1329–1334.
12 Larsen,T., Goodsell,D.S., Cascio,D., Grzeskowiak,K. and Dickerson,R.E. (1989) *J. Biomol. Struct. Dyn.*, **7**, 477–491.
13 Wang,A.H.-J. and Teng,M. (1990) In Bugg,C.E. and Ealick,S.E. (eds), *Crystallographic and Modeling Methods in Molecular Design*. Springer-Verlag, New York, NY, pp. 123–150.
14 Kopka,M.L. and Larsen,T.A. (1992) In Propst,C.L. and Perun,T.J. (eds), *Nucleic Acid Targeted Drug Design*. Marcel Dekker, Inc., New York, pp. 303–374.
15 Edwards,K.J., Jenkins,T.C. and Neidle,S. (1992) *Biochemistry*, **31**, 7104–7109.

16 Nunn,C.M., Jenkins,T.C. and Neidle,S. (1993) *Biochemistry*, **32**, 13838–13843.
17 Chen,X., Ramakrishnam,B., Rao,S.T. and Sundaralingam,M. (1994) *Nature Struct. Biol.*, **1**, 169–175.
18 Pelton,J.G. and Wemmer,D.E. (1989) *Proc. Natl Acad. Sci. USA*, **86**, 5723–5727.
19 Chen,X., Ramakrishnan,B. and Sundaralingam,M. (1997) *J. Mol. Biol.*, **267**, 1157–1170.
20 Chen,X., Ramakrishnan,B. and Sundaralingam,M. (1995) *Nature Struct. Biol.*, **2**, 733–735.
21 Wade,W.S., Mrksich,M. and Dervan,P.B. (1992) *J. Am. Chem. Soc.*, **114**, 8783–8792.
22 Mrksich,M. and Dervan,P.B. (1993) *J. Am. Chem. Soc.*, **115**, 9892–9897.
23 Kopka,M.L., Goodsell,D., Han,G.W., Chiu,T., Lown,J.W. and Dickerson,R.E. (1997) *Structure*, **5**, 1033–1046.
24 Kielkopf,C.L., Baird,E.E., Dervan,P.B. and Rees,D.C. (1998) *Nature Struct. Biol.*, **5**, 104–109.
25 Wang,B.C. (1985) *Methods Enzymol.*, **115**, 90–112.
26 Brunger,A.T. (1992) *X-PLOR Manual*, v.3.0. Yale University Press, New Haven, CT.
27 Chandrasekaran,R., Wang,M., Tang,M.-K., He,R.-G., Puigjaner,L.C., Byler,M.A., Millane,R.P. and Arnott,S. (1989) *J. Biomol. Struct. Dyn.*, **6**, 1189–1202.
28 Navaza,J. (1994) *Acta Crystallogr.*, **A50**, 157–160.
29 Brunger,A.T. (1992) *Nature*, **355**, 472–475.
30 Sack,J. and Quiocho,F.A. (1992) *CHAIN, Crystallographic Modelling Program*. Baylor College of Medicine, Houston, TX.
31 Berman,H.M., Olson,W.K., Beveridge,D., Westbrook,J., Gelbin,A., Demeny,T., Hsieh,S., Srinivasan,A.R. and Schneider,B. (1992) *Biophys. J.*, **63**, 751–759.
32 Sriram,M., van der Marel,G.A., Roelen,H.L.R.F., van Boom,J.H. and Wang,A.-H.J. (1992) *Biochemistry*, **31**, 11823–11834.
33 Bugg,C.E., Thomas,J.M., Sundaralingam,M. and Rao,S.T. (1971) *Biopolymers*, **10**, 175–219.
34 Wang,A.H.-J., Quigley,G.L., Kolpak,F.J., Crawford,J.L., van Boom,J.H., van der Marel,G. and Rich,A. (1979) *Nature*, **282**, 680–686.
35 Kopka,M.L., Goodsell,D.S., Baikalov,I., Grzeskowiak,K., Cascio,D. and Dickerson,R.E. (1994) *Biochemistry*, **33**, 13593–13610.
36 Fratini,A.V., Kopka,M.L., Drew,H.R. and Dickerson,R.E. (1982) *J. Biol. Chem.*, **257**, 14686–14707.